Numerical modeling of transverse mode competition in strongly pumped multimode fiber lasers and amplifiers

Mali Gong, Yanyang Yuan, Chen Li, Ping Yan, Haitao Zhang, Suying Liao

Center for Photonics and Electronics, State Key Laboratory of Tribology, Department of Precision Instruments, Tsinghua University, Beijing 100084, China
yuanyanyang@gmail.com

Abstract: A model based on propagation-rate equations with consideration of transverse gain distribution is built up to describe the transverse mode competition in strongly pumped multimode fiber lasers and amplifiers. An approximate practical numerical algorithm by multilayer method is presented. Based on the model and the numerical algorithm, the behaviors of multitransverse mode competition are demonstrated and individual transverse modes power distributions of output are simulated numerically for both fiber lasers and amplifiers under various conditions.

OCIS codes: (140.3510) Lasers, fiber; (060.2320) Fiber optics amplifiers and oscillators; (060.2280) Fiber design and fabrication; (060.2320) Nonlinear optics, fibers

References and links

1. Y. Jeong, J. K. Sahu, D. N. Payne, and J. Nilsson, "Ytterbium-doped large-core fiber laser with 1.36 kW continuous-wave output power," Opt. Express **12,** 6088-6092 (2004). http://www.opticsexpress.org/abstract.cfm?URI=OPEX-12-25-6088.
2. G. Bonati, H. Voelckel, T. Gabler, U. Krause, A. Tünnermann, J. Limpert, A. Liem, T. Schreiber, S. Nolte, and H. Zellmer, "1.53 kW from a single Yb-doped photonic crystal fiber laser," Photonics West, San Jose, Late Breaking Developments, Session 5709-2a (2005).
3. J. Limpert, S. Höfer, A. Liem, H. Zellmer, A. Tünnermann, S. Knoke, and H. Voelckel, "100-W average-power, high-energy nanosecond fiber amplifier," Appl. Phys. B: Lasers & Optics **75**, 477-479 (2002).
4. J.P. Koplow, D.A. V. Kliner, and L. Goldberg, "Single-mode operation of a coiled multimode fiber amplifier," Opt. Lett. **25**, 442-444 (2000).
5. M.D. Nielsen, N.A. Mortensen, M. Albersen, J.R. Folkenberg, A. Bjarklev, and D. Bonacinni, "Predicting macrobending loss for large-mode area photonic crystal fibers," Opt. Express **12**, 1775 (2004) http://www.opticsexpress.org/abstract.cfm?URI=OPEX-12-8-1775
6. A. Hardy and R. Oron, "Signal amplification in strongly pumped fiber amplifiers," IEEE J. Quantum Electron. **33**, 307-313 (1997).
7. I. Kelson and A. A. Hardy, "Strongly pumped fiber lasers," IEEE J. Quantum Electron. **34**, 1570–1577 (1998).
8. J.Limpert, H.Zellmer, and A. Tünnermann, "Suppression of high order modes in a multimode fiber amplifier using efficient gain-loss-management (GLM)," in *Advanced Solid-State Lasers*, Québec City, Canada, paper MB20, 112-114, 2002.
9. M. Hotoleanu, M. Söderlund, D. Kliner, J. Koplow, S. Tammela, and V. Philipov, "High order modes suppression in large mode area active fibers by controlling the radial distribution of the rare earth dopant," In Fiber Lasers III, A.J.W. Brow, J. Nilsson, D.J. Harter, A. Tünnermann, eds., Proc. SPIE **6102,** 61021T1-61021T8 (2006).
10. T. Bhutta, J. I. Mackenzie, D. P. Shepherd, and R. J. Beach, "Spatial dopant profiles for transverse-mode selection in multimode waveguides," J. Opt. Soc. Am. B, **19**, 1539-1543 (2002).
11. A.Galvanauskas, "Mode-Scalable Fiber-Based Chirped Pulse Amplification Systems," IEEE J. Sel. Top. Quantum Electron.**7,** 504-517 (2001).
12. R. Paschotta, J. Nilsson, A. C. Tropper, and D. C. Hanna, "Ytterbium doped fiber amplifiers," IEEE J. Quantum Electron. **33**, 1049–1056 (1997).
13. D. Marcuse, "Curvature loss formula for optical fibers," J. Opt. Soc. Am. **66,** 216-220 (1976).

#78822 - $15.00 USD Received 9 January 2007; revised 4 March 2007; accepted 5 March 2007

1. Introduction

Rare-earth-doped fiber lasers and amplifiers reveal a number of benefits in terms of outstanding thermo-optical properties, high conversion efficiency, excellent beam quality and good compactness compared with the traditional solid-state laser systems. In the recent years, rapid advances in fiber and laser diode technologies have led to kilowatt CW fiber lasers with output beams of single transverse mode quality [1,2] and multi-mJ Q-switched fiber lasers with diffraction-limited beam quality ($M^2 = 1.1$) [3].

However, a further power/energy scaling of fiber lasers or amplifiers is mainly limited by the detrimental effects of various nonlinear processes in fibers such as stimulated Brillouin scattering (SBS), stimulated Raman scattering (SRS) and self-phase modulation (SPM). In general, these nonlinear effects mentioned above scale with the fiber length and are inversely proportional to the mode-field-area of the fiber core. As a result, an effective solution to this problem is to adopt large mode area (LMA) fiber with high doping concentration. But increasing the core size of a fiber eventually will allow it to support more spatial modes which will degrade the beam quality of the laser output. Usually, there are two ways to achieve large mode area fiber while still maintaining in the single mode regime. The most common way is to use multimode fiber with the aid of mode selection technique. Several research groups have suppressed the excitation or propagation of high order transverse modes in multimode fibers by suitably designing the fiber index, tailoring the dopant profiles, coiling the fiber, introducing special cavity configurations, tapering the fiber ends, or carefully adjusting the launch conditions of a seed beam [4]. An alternative way is to use photonic crystal fiber (PCF). The most attractive advantage of PCFs is their endlessly single-mode property combined with unlimited large effective areas in principle, but the bending sensitivity and propagation losses will increase with the enlargement of the fiber core [5].

In this paper, we do pay attention to the former way. In multimode fiber lasers or amplifiers, each potential transverse mode is possible to be excited and propagate because transverse spatial hole burning and mode coupling effects. When we concern some special transverse mode (especially fundamental mode), the mode selection techniques mentioned above will be applied. In any case, the transverse mode competition exists inside the fiber and affects the intensity distribution of output. However, few literatures discuss this behavior in the fiber lasers and amplifiers. References [6,7] have analyzed the strongly pumped fiber amplifiers and lasers in detail, where a single mode fiber is assumed and transverse gain is not considered. References [8-10] have investigated transverse mode discrimination in multimode fibers by spatially controlling the radial dopant distribution, where relative gain of transverse modes in fibers was calculated for mode selection, but the model for describing the behaviors of transverse mode competition and the output power distribution of each mode were not discussed. The goal of this paper is to introduce a model for describing the transverse mode competition in strongly pumped fiber lasers and amplifiers with or without the various mode selection techniques. The model is based on a set of rate equations, in which the interaction between multitransverse modes and active dopant in both transverse and longitudinal directions was considered. An approximate practical numerical algorithm with multilayer method is presented, which makes the equations easy to be solved. Based on the model and the numerical algorithm, the behaviors of transverse mode competition are demonstrated and individual transverse mode power distributions of output are simulated for both fiber lasers and amplifiers under various conditions.

2. Theoretical Model

When analyzing the transverse mode competition in the multimode fiber lasers, it is necessary to present the gain distribution in the transverse direction of the fiber. Each transverse mode has individual field intensity distribution, which interacts with the population inversion and shares it. In the competition by sharing the population inversion, the transverse mode which obtains enough gains will be excited and propagate.

#78822 - $15.00 USD Received 9 January 2007; revised 4 March 2007; accepted 5 March 2007

The model of fiber lasers that has been developed uses the typical linear cavity as described schematically in Fig. 1. The case of amplifiers is similar except to remove two reflectors.

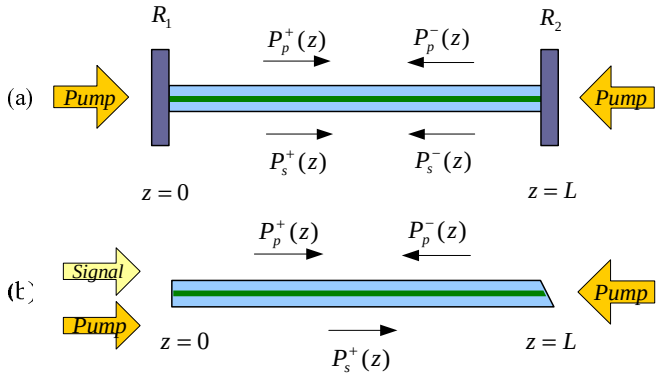

Fig. 1. Schematic illustration of the model: (a) fiber lasers (b) fiber amplifiers.

In this model , the following assumptions are made: (1) two-level systems are considered where the excited state absorption (ESA) is neglected; (2) for a strongly pumped multimode fiber, the pump light is assumed to be homogeneous over the cross section of the fiber cladding and the amplified spontaneous emission (ASE) are ignored; (3) the polarization effects and interactions between neighboring ions (e.g. clustering) are ignored; (4) only one single longitudinal mode is assumed in the fiber.

2.1 Rate Equations

When considering the interaction between the active dopant and each potential transverse mode, the population inversion distribution is not constant in the transverse direction any more. Based on the rate equations presented in Ref. [7] and the assumptions above, the model we developed here to describe the transverse mode competition in multimode fiber lasers and amplifiers can be expressed by the following space-dependent and time-independent steady-state rate equations:

$$\frac{N_2(r,\varphi,z)}{N_1(r,\varphi,z)}=\frac{\dfrac{[P_p^+(z)+P_p^-(z)]\sigma_{ap}\Gamma_p(r,\varphi)}{h\nu_p}+\sum_i\dfrac{[P_{si}^+(z)+P_{si}^-(z)]\sigma_{as}\Gamma_{si}(r,\varphi)}{h\nu_s}}{\dfrac{[P_p^+(z)+P_p^-(z)]\sigma_{ep}\Gamma_p(r,\varphi)}{h\nu_p}+\dfrac{1}{\tau}+\sum_i\dfrac{[P_{si}^+(z)+P_{si}^-(z)]\sigma_{es}\Gamma_{si}(r,\varphi)}{h\nu_s}} \tag{1}$$

$$\pm\frac{dP_p^{\pm}(z)}{dz}=\left\{\int_0^{2\pi}\int_0^a\left[\sigma_{ep}N_2(r,\varphi,z)-\sigma_{ap}N_1(r,\varphi,z)\right]\Gamma_p(r,\varphi)rdrd\varphi\right\}P_p^{\pm}(z)-\alpha_pP_p^{\pm}(z) \tag{2}$$

$$\pm\frac{dP_{si}^{\pm}(z)}{dz}=\left\{\int_0^{2\pi}\int_0^a\left[\sigma_{es}N_2(r,\varphi,z)-\sigma_{as}N_1(r,\varphi,z)\right]\Gamma_{si}(r,\varphi)rdrd\varphi\right\}P_{si}^{\pm}(z)-\alpha_{si}P_{si}^{\pm}(z)-\sum_j d_{ij}[P_{si}^{\pm}(z)-P_{sj}^{\pm}(z)] \tag{3}$$

where h is Planck constant; τ is the spontaneous lifetime of the upper lasing level; ν_p and ν_s are pump and signal frequencies; a is the radius of the fiber core; $N_1(r,\varphi,z)$ and $N_2(r,\varphi,z)$ are the population densities of the lower and upper lasing levels at the position (r,φ,z) ($N(r,\varphi,z)=N_1(r,\varphi,z)+N_2(r,\varphi,z)$ is the doping concentration distribution which is constant along the fiber axis and has a radial symmetry), respectively; $P_p^+(z)$ and $P_p^-(z)$ are the pump powers in the forward and backward directions, respectively; $P_{si}^+(z)$ and $P_{si}^-(z)$ are the signal

#78822 - $15.00 USD Received 9 January 2007; revised 4 March 2007; accepted 5 March 2007

powers of the i^{th} transverse mode in the forward and backward directions, respectively; $\sigma_{ap}(\sigma_{ep})$ and $\sigma_{as}(\sigma_{es})$ are the pump absorption(emission) and signal absorption(emission) cross-sections, respectively; α_p and α_{si} are the pump and signal of the i^{th} mode loss factors; d_{ij} is the power coupling coefficient between the i^{th} mode and the j^{th} mode; $\Gamma_p(r,\varphi)$ and $\Gamma_{si}(r,\varphi)$ are the pump and signal of the i^{th} mode power filling distributions which can be expressed as follows:

$$\Gamma_p(r,\varphi)=\frac{1}{A_{clad}},\ \int_0^{2\pi}\int_0^{a}\Gamma_p(r,\varphi)rdrd\varphi=\Gamma_p=\frac{A_{core}}{A_{clad}} \tag{4}$$

$$\Gamma_{si}(r,\varphi)=\frac{\psi_i(r,\varphi)}{\int_0^{2\pi}\int_0^{\infty}r\psi_i(r,\varphi)drd\varphi},\ \int_0^{2\pi}\int_0^{a}\Gamma_{si}(r,\varphi)rdrd\varphi=\Gamma_{si}=\frac{P_i^{core}}{P_i^{core}+P_i^{clad}} \tag{5}$$

where $\psi_i(r,\varphi)$ denotes the distribution function of the i^{th} mode intensity; A_{core} and A_{clad} are the areas of core and inner cladding respectively. Eq. (1) expresses the ground-state and excited-state population densities $N_1(r,\varphi,z)$ and $N_2(r,\varphi,z)$ that varies with the forward and the backward directions of the signal powers of the i^{th} mode $P_{si}^{\pm}(z)$ as well as the pump powers $P_p^{\pm}(z)$ at the same location. Equations (2) and (3) describe the pump and signal (each individual transverse mode) power evolution along the fiber length. In our model, the cross-coupling between modes is also considered which will result in mode conversion and also affect the output intensity distribution [11].

2.2 Multilayered method for numerical simulations

The theoretical model for describing the mode competition in multimode fibers is given by Eqs. (1)-(5) completely. But commonly, it is difficult to solve these complicated equations due to the integrations in Eqs. (2) and (3). Here we present an alternative approximate approach. It is to divide the cross section of the fiber core into a finite number of distinctive layers (as shown in Fig. 2), each of which is thin enough so that the dopant concentration and the population inversion can be deemed as a constant. This division is reasonable for the index and dopant profiles have circular symmetries in most cases. Obviously, the accuracy of this method depends on the number of divided layers M. In our simulations, we found that there is a good balance between the accuracy and the computing time when $M=100$. By applying this method, the Eqs. (1)-(5) can be replaced by the following set of simplified equations:

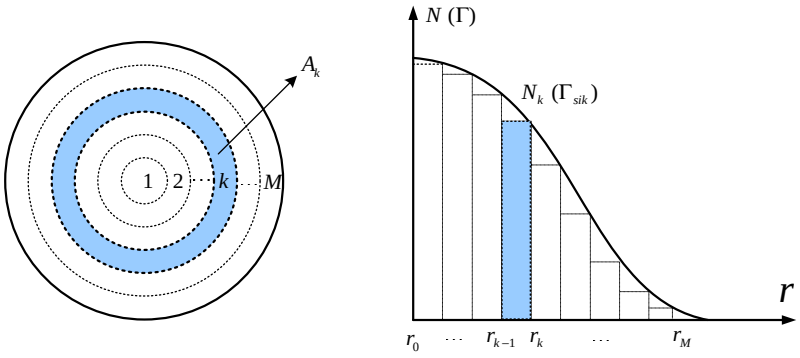

Fig. 2. Illustration of multilayered method (M layers divided).

#78822 - $15.00 USD Received 9 January 2007; revised 4 March 2007; accepted 5 March 2007

$$\frac{N_{2k}(z)}{N_{1k}(z)}=\frac{\dfrac{[P_p^+(z)+P_p^-(z)]\sigma_{ap}\Gamma_{pk}}{h\nu_p A_k}+\sum_i\dfrac{[P_{si}^+(z)+P_{si}^-(z)]\sigma_{as}\Gamma_{sik}}{h\nu_s A_k}}{\dfrac{[P_p^+(z)+P_p^-(z)]\sigma_{ep}\Gamma_{pk}}{h\nu_p A_k}+\dfrac{1}{\tau}+\sum_i\dfrac{[P_{si}^+(z)+P_{si}^-(z)]\sigma_{es}\Gamma_{sik}}{h\nu_s A_k}}\ (k=1,2,\cdots,M) \tag{6}$$

$$\pm\frac{dP_p^{\pm}(z)}{dz}=\sum_k\Gamma_{pk}[\sigma_{ep}N_{2k}(z)-\sigma_{ap}N_{1k}]P_p^{\pm}(z)-\alpha_p P_p^{\pm}(z) \tag{7}$$

$$\pm\frac{dP_{si}^{\pm}(z)}{dz}=\sum_k\Gamma_{sik}[\sigma_{es}N_{2k}(z)-\sigma_{as}N_{1k}]P_{si}^{\pm}(z)-\alpha_{si}P_{si}^{\pm}(z)-\sum_j d_{ij}[P_{si}^{\pm}(z)-P_{sj}^{\pm}(z)] \tag{8}$$

$$\Gamma_{pk}=\frac{A_k}{A_{clad}},\Gamma_{sik}=\frac{\int_{r_{k-1}}^{r_k}\int_0^{2\pi}r\psi_i(r,\varphi)drd\varphi}{\int_0^{\infty}\int_0^{2\pi}r\psi_i(r,\varphi)drd\varphi} \tag{9}$$

where $A_k=\pi(r_k^2-r_{k-1}^2)\ (k=1,2,\cdots,M;r_0=0)$ is the area of the k^{th} layer; Γ_{pk} and Γ_{sik} are the pump and signal power filling factors in the k^{th} layer. In a step index multimode fiber, the Γ_{sik} can be given by

$$\Gamma_{sik}=\frac{\left(\frac{r_{k-1}}{a}\right)^2\left[J_m(U\frac{r_{k-1}}{a})^2-J_{m-1}(U\frac{r_{k-1}}{a})J_{m+1}(U\frac{r_{k-1}}{a})\right]-\left(\frac{r_k}{a}\right)^2\left[J_m(U\frac{r_k}{a})^2-J_{m-1}(U\frac{r_k}{a})J_{m+1}(U\frac{r_k}{a})\right]}{\frac{V^2}{V^2-U^2}J_{m-1}(U)J_{m+1}(U)} \tag{10}$$

where *V* and *U* are, respectively, the normalized frequency and transverse wave numbers. For N number of modes and *M* number of layers, the total number of coupled equations is $M+2N+2$. It should be pointed out that, for LP_{mn} mode, those modes where $m\neq 0$ must be calculated twice in Eq (8) for having two helical polarities (LP_{mn}^c and LP_{mn}^s).

2.3 Boundary and initial conditions

To solve the coupled differential Eqs. (6)-(8), additional boundary or initial conditions are needed. For fiber lasers, the boundary conditions are given by

$$P_{si}^+(0)=R_1P_{si}^-(0) \tag{11}$$

$$P_{si}^-(L)=R_2P_{si}^+(L) \tag{12}$$

where L is the fiber Length; R_1 and R_2 are the reflectivities of the reflectors at $z=0$ and $z=L$, respectively. At the beginning of the simulation, an initial guess for each transverse mode is given, and Eqs. (6)-(8) are iterated until the output power $P_{si}^{out}=(1-R_2)P_{si}^+(L)$ convergences. For fiber amplifiers, usually, both the pump and signal propagate in only one direction (the corresponding items in Eqs. (6)-(8) can be omitted). In the case of a copropagating signal, giving the initial pump and signal power at $z=0$, the evolution of the signal powers can be calculated straightforward from the input end to the output end by using the forth-order Runge-Kutta method. A counterpropagating signal is a little more complicated. In which case, an estimate for the output signal power from the pump end to the other end, refining the estimate in an iterative procedure until the given signal input power is reproduced by the calculation at this end.

3. Numerical simulation results and discussion

Based on the discussion presented above, the theoretical model and the corresponding numerical algorithm were built up. In this section, we simulated the behaviors of transverse

#78822 - $15.00 USD Received 9 January 2007; revised 4 March 2007; accepted 5 March 2007

mode competition in Yb-doped multimode fiber amplifiers and lasers respectively under various conditions, such as various dopant distributions, pump powers and discriminative loss factors for different transverse mode. All of the mode selection techniques mentioned at the beginning of this paper can be included in these cases. In the following simulations, the traditional step index multimode fiber was taken into consideration, and other kinds of fibers can be treated similarly. In addition, we considered the mode competition in a perfectly flawless multimode fiber without any other external disturbance, so the power coupling coefficient d_{ij} in Eq. (8) is neglected. The parameters employed in the numerical simulations are listed in Tab. 1.

Table 1. Parameters used for simulations of Yb-doped fiber lasers and amplifiers

Parameter	Value	Parameter	Value
D_{core} (μm)	28	λ_p (nm)	975
D_{clad} (μm)	500	λ_s (nm)	1064
NA_{core}	0.06	σ_{ap} (cm^2)	2.5×10^{-20}
N_{amp} (cm^{-3})	1.3×10^{20}	σ_{ep} (cm^2)	2.5×10^{-20}
N_{laser} (cm^{-3})	4.6×10^{19}	σ_{as} (cm^2)	6.4×10^{-23} [12]
R_1	0.99	σ_{es} (cm^2)	3.2×10^{-21} [12]
R_2	0.04	α_p (cm^{-1})	2×10^{-5}
τ (ms)	0.8	α_s (cm^{-1})	4×10^{-6}

First, by using this model, we simulated the power propagation of each mode in fiber amplifiers with various dopant distributions which was demonstrated in Ref. [9]. The simulated results are shown in Fig. 3, where Γ is the doping confinement factor defined as the ratio of the maximum gain radius to the core radius and ρ denotes the normalized radius. In order to describe the competition of every potential mode during propagation, 50W pump power and 100mW initial copropagated signal power for each mode are given. The fiber lengths have been calculated until the amplified signal power is close to the maximum possible in each case. For flat doping fibers (Fig. 3(a)-(c)), when $\Gamma=1$ (in most common cases), the first high order mode LP_{11} has the maximum output. The output power of LP_{01}, LP_{11}, LP_{21} and LP_{02} are 8.9W, 16.2W, 12.4W and 4.4W respectively. The percentage of the fundamental mode (LP_{01}) output in total rises from 21.3% ($\Gamma=1$) to 54.5% ($\Gamma=0.75$) and 78.5% ($\Gamma=0.5$). From Fig. 3(c), we can see that the output of LP_{02} has exceeded LP_{11} and LP_{21} when $\Gamma=0.5$. All of these indicate that small Γ favors the modes which have more power concentrated in the center of the core. However, Γ could not be too small for ensuring more gain to the LP_{01} than LP_{02}. Figure 3(d) shows the parabolic doping fibers can also favor the LP_{01} which raise the percentage of the LP_{01} to 48.5%. The dependence of the power faction of LP_{01} mode on doping confinement factor in the flat doping fibers is shown in Fig. 4. We calculated four modes ($LP_{01,}$ $LP_{11,}$ LP_{21} and LP_{02}) in the fibers with different core diameters (28, 50 and $100\mu m$) at 100W pump power. It signifies that the optimized doping confinement factor is around 0.5~0.6. It also indicates that it is possible to achieve single transverse mode output even when the core diameter is up to $100\mu m$ by further optimizing the doping profile and highest doping concentration.

Figure 5 illustrates the power propagation of each guided mode in fiber amplifiers with discriminative loss factors which are realized by coiling the fiber. The bending-loss factors in Fig.5 are derived from the analysis of Marcuse in Ref. [13]. It can be seen that when bending

#78822 - $15.00 USD Received 9 January 2007; revised 4 March 2007; accepted 5 March 2007

radius is $7.5\,cm$, there are two modes (LP_{01} and LP_{11}) propagating in the fiber with a certain length. The output power of LP_{11} decreases slowly with the increase of the fiber length and the maximum LP_{01} output power is 17W. And when bending radius is reduced to $6\,cm$, only LP_{01}

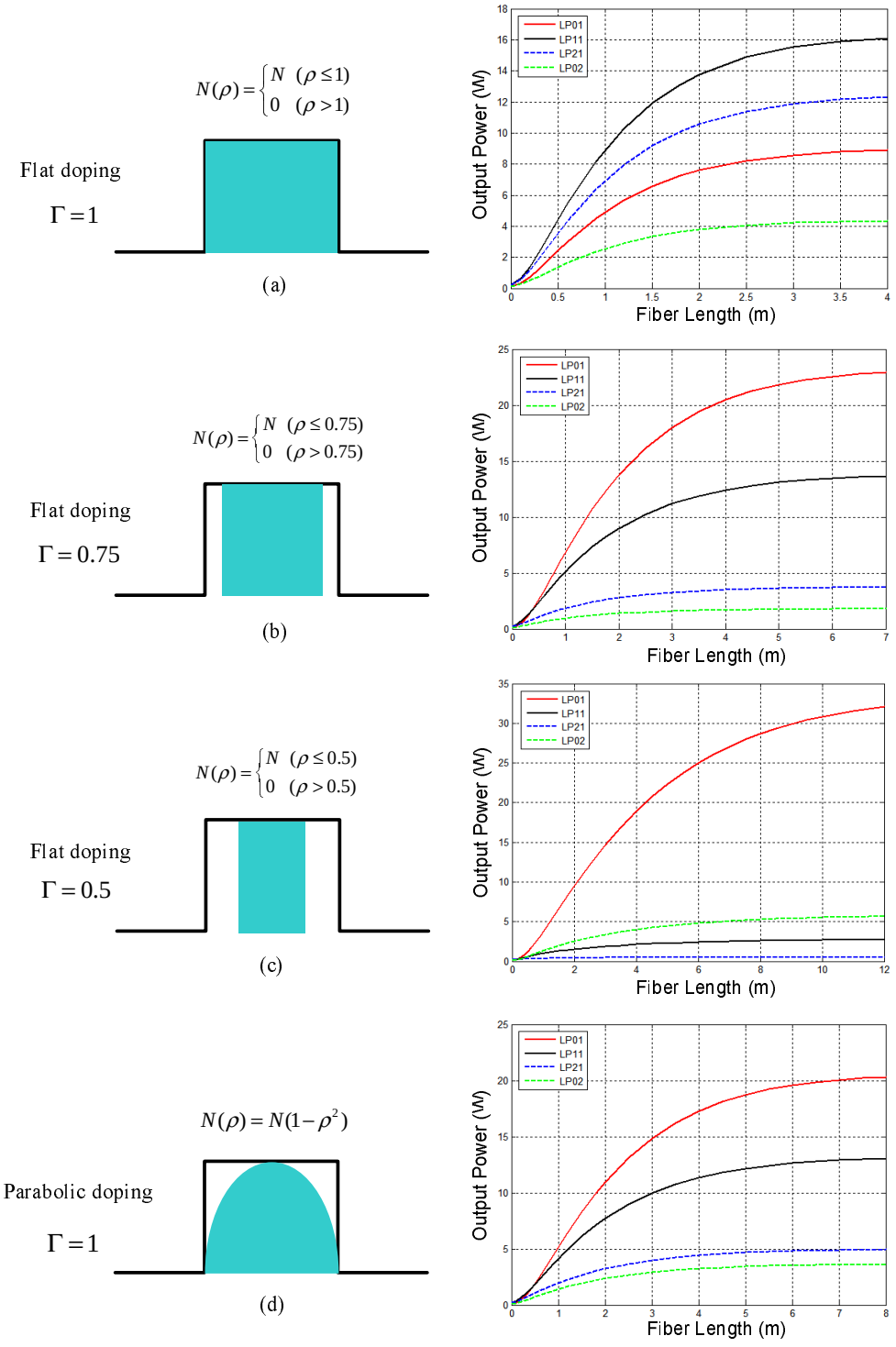

Fig. 3. Power propagation of each mode in fiber amplifiers with various dopant profiles .

#78822 - $15.00 USD
Received 9 January 2007; revised 4 March 2007; accepted 5 March 2007

mode remained in the fiber for the strong suppression of the high order modes. In this case, the output power of LP_{01} is 37W which is much more than the former, because the power of LP_{11} drops quickly and LP_{01} monopolizes the gain in the fiber.

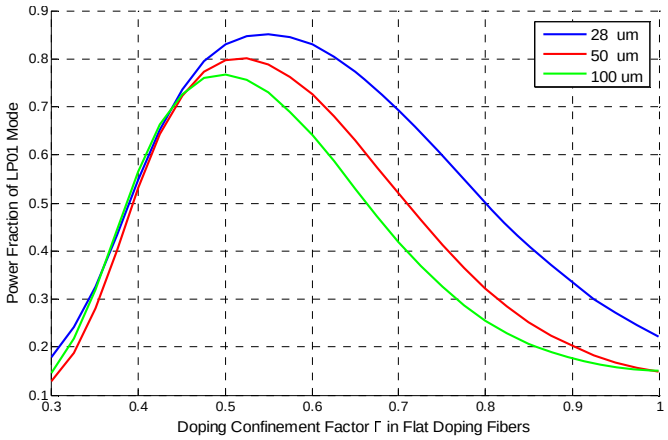

Fig. 4. Power faction of LP_{01} mode versus doping confinement factor in flat doping fibers with different core diameters (28, 50 and 100 um).

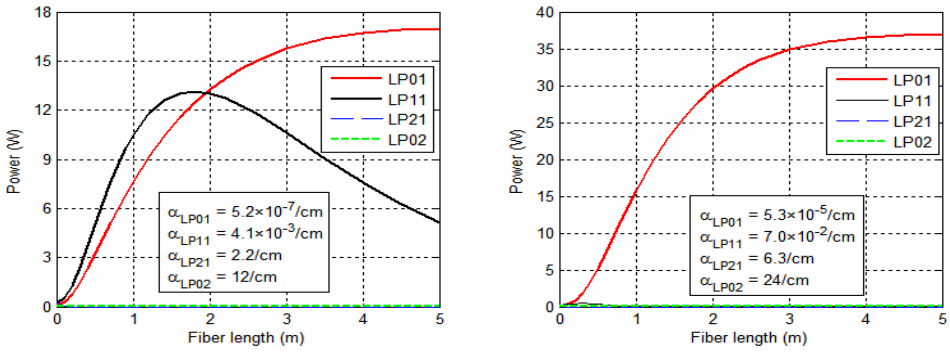

(a) 7.5cm bending radius (b) 6cm bending radius

Fig. 5. Power propagation of each mode in fiber amplifiers with discriminative loss factors .

Figure 6 illustrates the power distribution of each mode varied with the pump powers in flat-doping fiber lasers with $\Gamma = 1$. The fiber with 10m length was pumped equally at double ends. The right sub-figure in Fig. 6 is the details of the left one at low pump power. It can be seen that not all of potential modes could be excited at one time in the fiber lasers. When the pump power is low, only LP_{01} mode is preferentially excited due to its lower threshold. The high order modes LP_{11} and LP_{21} are excited successively with the increase of pump power. Then, the outputs of all excited modes increase linearly above their respective threshold pump powers. The LP_{11} has maximum output and the percentages of these excited modes are 30% (for LP_{01}), 45% (for LP_{11}) and 25% (for LP_{21}) respectively at high pump power.

#78822 - $15.00 USD Received 9 January 2007; revised 4 March 2007; accepted 5 March 2007

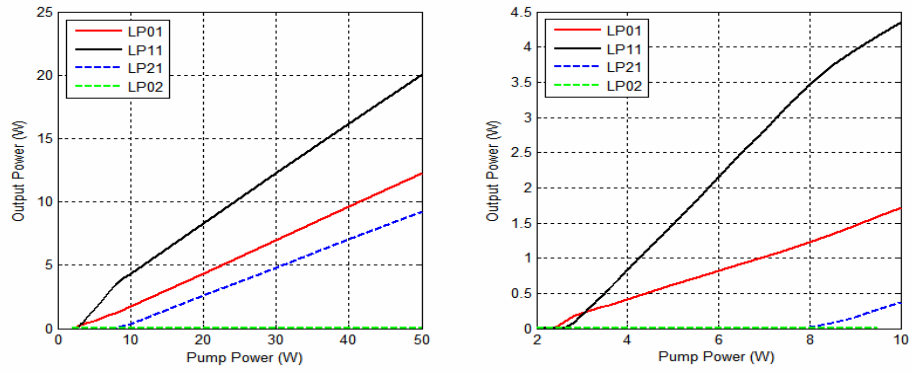

Fig. 6. Power distribution of each mode in fiber lasers varied with pump powers in flat-doping fiber lasers with $\Gamma = 1$.

Figure 7 shows the transverse gain distributions (N_2 / N) at the output end of the fiber with different pump powers. It indicates that the gain varies along the radial direction because of transverse mode competition in the fibers. When the pump is low and only LP_{01} is excited, the gain is lowest in the center and increases with the radial position which is opposite to the intensity distribution of LP_{01} mode, arising from the effect of gain saturation. With the increase of pump power, the gain curve drops and the valley point on it shifts away from the center for the high order modes (LP_{11} and LP_{21}) account for more and more fraction of the output.

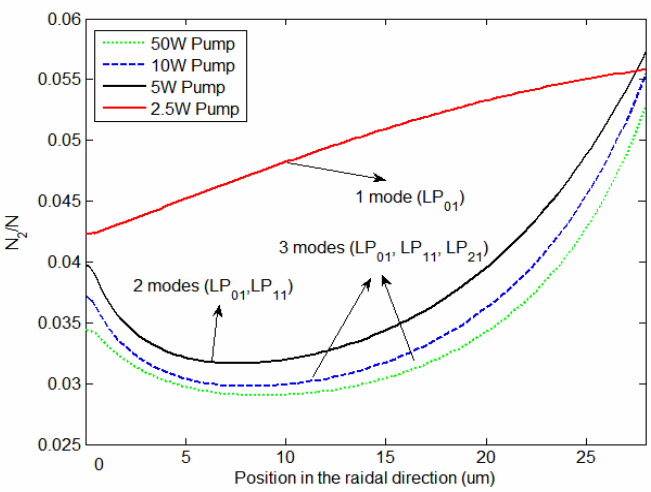

Fig. 7. Transverse gain distributions at the output end with different pump powers.

We have also simulated the output power distributions in the fiber lasers with various dopant profiles and discriminative loss factors which are shown in Fig. 8. It can be seen that, as similar as the case of fiber amplifiers, decreasing the doping confinement factor Γ or parabolic doping or coiling the fibers with appropriate bending radius can favor the LP_{01} mode and even achieve single mode output in this fiber with low NA. Differently, the mode competition in the fiber lasers is more serious because of the laser cavity configurations.

#78822 - $15.00 USD Received 9 January 2007; revised 4 March 2007; accepted 5 March 2007

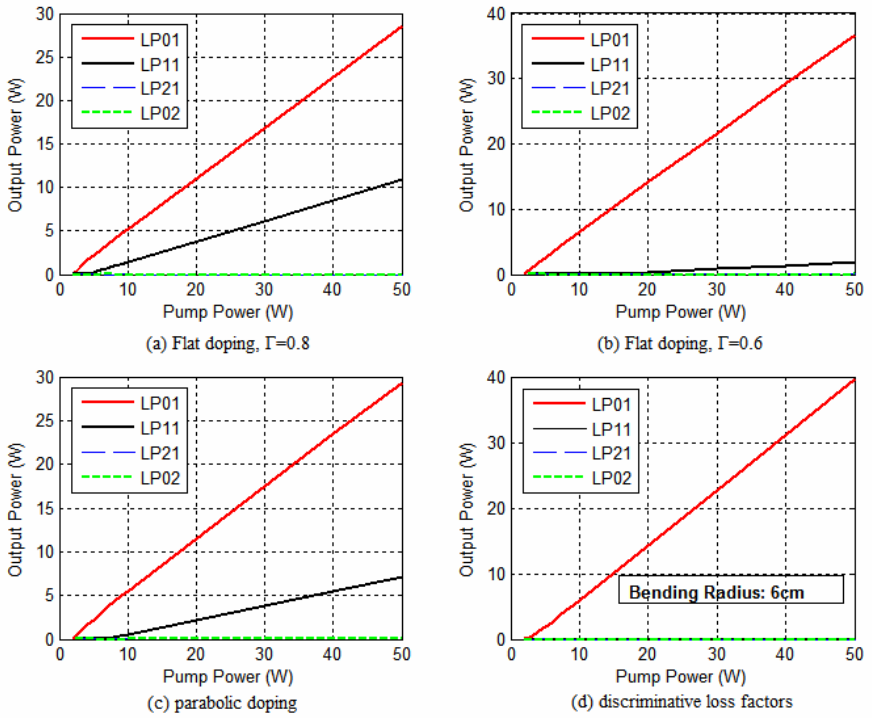

Fig. 8. Output power distributions of each mode in fiber lasers with various dopant profiles and discriminative loss factors.

The simulations above present the transverse mode competition in the multimode fibers without applying the cross-couple between the modes, because it is hard to determine the mode coupling matrix d_{ij}, although we have considered this effect in our model. The mode coupling in multimode fibers is a very complex problem which is caused by many uncertain factors, mainly including the internal flaw generated during the fabrication procedure and other external disturbance such as bending, twisting, and etc. In order to exhibit our model has the ability to process this case, here, we give a simple example to reveal the mode coupling effect between the fundamental mode LP_{01} and the closest higher order mode LP_{11}. Figure 9 shows the power fraction of LP_{01} mode varies the fiber length in a fiber laser with different mode coupling coefficients between these two modes. The fiber core diameter is 18 μm and inner cladding diameter is 200 μm and other simulation parameters are as same as those in Tab. 1. The mode coupling coefficient From Fig. 9, it can be seen that the mode coupling has important effect on the output intensity distribution, especially in a long fiber. When the fiber length is in the range of several meters, the LP_{01} mode fraction drops about 20 percent for d=0.01/m (the value is from Ref. 11) and about 5 percent for d=0.001/m. So if more accurate output intensity distribution is needed, further study on mode coupling effect should be taken into account.

#78822 - $15.00 USD Received 9 January 2007; revised 4 March 2007; accepted 5 March 2007

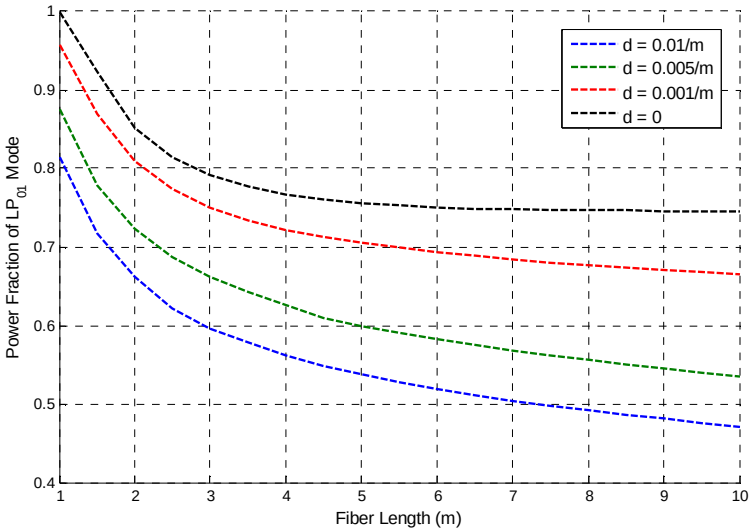

Fig. 9. Power faction of LP_{01} mode varies fiber length with different mode coupling coefficients in a two mode fiber lasers.

4. Conclusion

In this paper, a model for describing the transverse mode competition in strongly pumped fiber lasers and amplifiers with or without the mode selection techniques was built up. The model is based on rate equations, in which the interaction between multitransverse modes and active dopant in both transverse and longitudinal directions was considered. In the model, the mode cross-coupling effect was also considered. A practical numerical algorithm with multilayer method was also presented which makes the equations easy to be solved.

Based on the model and the numerical algorithm, the behaviors of multitransverse mode competition were demonstrated and individual transverse modes power distributions of output were simulated numerically in both fiber lasers and amplifiers with various dopant distributions, pump powers and loss factors. The cross-coupling effect between only two modes was also discussed. In the simulations, the traditional step index multimode fiber was taken into consideration, but this model is also applicable for other kinds of multimode fibers (e.g. PCFs). This model could be helpful for designing large mode area fibers, especially for designing such fibers by means of optimizing index and dopant profiles of the fiber, and also could be useful to evaluate the beam quality of multimode fiber lasers.

#78822 - $15.00 USD Received 9 January 2007; revised 4 March 2007; accepted 5 March 2007